



Thermal strength of the alkali-activated slag concrete

M. Shahbaz^{1*}, K. Behfarnia²

¹Department of Civil Engineering, University of Isfahan, Isfahan, Iran

²Department of Civil Engineering, Isfahan University of Technology, Isfahan, Iran

ABSTRACT: Every structure may experience elevated temperatures during its service life. Heat changes the physical and mechanical properties of concrete. The increasing need for cement for concrete preparation has had an environmental impact including about 7% share of CO₂ emissions to the atmosphere. Thus, it is essential to provide alternative products to move on the path of sustainable development to reduce these effects. One of the strategies for environmentally friendly concrete production is to use alkali-activated slag concrete (AASC). Alkali-activated slag (AAS), if designed properly, could be considered as a proper replacement for Portland cement. In this study, alkali-activated slag concrete specimens with different slag contents were placed in a furnace at different temperatures up to 800°C. The effect of temperature on the mass loss and the compressive strength of the AAS concrete was investigated. Portland cement specimens were also prepared to be compared with the AAS concrete ones. The data was analyzed using the T-test method, as well as one-way and two-way ANOVA. Finally, scanning electron microscopy images were used to compare the microstructures of the concrete at different temperatures and the pore structure of AAS concrete was investigated using mercury intrusion porosimetry. Overall, the results showed the very good thermal performance of the AAS concrete in comparison with that of the Portland cement one

Review History:

Received: 2019-07-19

Revised: 2019-08-20

Accepted: 2019-12-20

Available Online: 2019-12-25

Keywords:

Alkali-activated concrete

Slag

Mass loss

Compressive strength

Thermal performance

Statistic analysis

SEM

MIP

1. INTRODUCTION

It is inevitable to pay special attention to the environmental impact of cement production and power consumption in the form of electricity and fossil fuels. Accordingly, it is essential to provide alternative products to the pursuit of sustainable development and to reduce these effects. Therefore, in recent years, materials with aluminosilicate bases (which are often considered by-products of the industries) are known as an alternative of cement. These materials cause adhesion due to the reaction with alkali activators, known as 'alkali-activated material (AAM)', and extensive research is ongoing on these cement-like binders [1-4]. Slag, as an alkali-activated material, has received attention due to the high percentage of calcium (CaO); it is chemically similar to the normal Portland cement and produces the concrete called 'alkali-activated slag concrete (AASC)'. It can be considered as a proper alternative to the normal concrete [5, 6]. The main reaction product in the alkali-activated material, which is tobermorite-like in structure, is calcium aluminum silicate hydrate (C-A-S-H) gel [7].

In recent years, the study of the effect of heat on the alkali-activated concrete has been investigated by researchers; accordingly, they have addressed the effects of ductility and transit creep on the residual strength [8-10], the residual

strength of the alkali-activated slag concrete [11], and the spalling of geopolymer and Portland cement concrete in the simulated fire [12]; they have also concerned with the effects of the specimen size, aggregate size, aggregate type, precursors, and activators on the thermal properties [13-15]. Ceramic properties of AAS concrete due to aluminate silicate compounds have made the AAS concrete more heat resistant than normal concrete [16]. The thermal resistance of the alkali-activated concrete with fly ash up to 1200°C was investigated. Concrete produced with potassium silicate showed higher thermal resistance than concrete made with sodium hydroxide, which is due to the fact that potassium silicate significantly reduces the pore size in paste [17]. The amount of K₂O in an alkali-activated binder is very important. The increase in K₂O can raise the setting time, the compressive strength, and the thermal properties of the alkali-activated concrete [18]. Based on the researches, Bentonite Geopolymer has the highest heat resistance, while FeNi Slag geopolymer displays the least one [19]. A recent study showed that AAS samples lost 65% of their compressive strength at 800°C [20]. The compressive strength of heavyweight geopolymer concrete increases with increasing temperature but decreases at 600°C and 900°C [21]. AAS concrete samples lose 10% of their tensile strength up to 200°C while at 600°C, about 85% of the tensile strength of the specimens is lost [22]. The decline in strength is caused by the different thermal

*Corresponding author's email: mohammad.shahbaz16@yahoo.com



expansion between the geopolymer and aggregates. Separate dilatometry tests show that while aggregates are expanding at the elevated temperatures, the geopolymer matrix experiences contraction [13]. Aggregate size plays an important role in the thermal resistance of geopolymer concrete. Concretes containing aggregates larger than 10 mm in size show better stability at high temperatures and aggregates smaller than 10 mm improve spalling and extensive cracking [14]. Cracks created in the slag paste caused by temperature gradient, pores pressure, and phase changes at high-temperatures are the main reason for the degradation of mechanical properties. On the other hand, the main mechanism accounting for the degradation of the mechanical properties of concrete is the thermal expansion incompatibility between the contraction of the paste matrix and the expansion of aggregates [23].

The aim of this study was, therefore, to investigate the mass loss and compressive strength variations of AASC containing varying amounts of the blast furnace slag after heating at 20, 200, 400, 600 and 800 °C. For this purpose, all specimens, after 7 and 28 days of wet curing, were subjected to the elevated temperatures in a fossil-fuel-fired (gas-fired) furnace. After cooling the specimens at the ambient temperature, the changes in the mass and compressive strength of the AAS and normal concrete were measured. The data was analyzed using the T-test method, as well as one-way and two-way ANOVA, with the significance level of 0.05. So far, less research has been concerned with both alkali-activated slag and normal concrete constructed with a similar mix design and cured in the same conditions. So, further research could provide a complete and comparable picture regarding the thermal performance of these two types of concrete. The changes in the microstructure and porosity of the alkali-activated slag and cement pastes due to high temperature were studied by scanning electron microscopy (SEM) images and mercury intrusion porosimetry (MIP), respectively.

2. EXPERIMENTAL INVESTIGATION

2.1. Materials

Slag is the main binder in the alkali-activated slag concrete. In this study, Esfahan Steel Company (ESC) blast furnace slag

(in the form of granules) was used according to the analysis presented in Table 1. The SO₃ content in slag according to ASTM C989M-13 [24] was limited to 4%. This was about 2.4% in the slag. Regardless of the slag chemical composition, if Al₂O₃/SiO₂ varies from 0.1 to 0.6, the slag can be well used for AASC production [25]. According to the specifications of the slag used in this study, Al₂O₃/SiO₂ was equal to 0.375. To ensure proper slag hydration, the slag hydration modulus should be more than 1.4 [26]. Its hydration modulus (HM = (CaO + MgO + Al₂O₃)/SiO₂) was 1.7. The specific gravity and blaine of the slag were equal to 2.8 and 4500 cm²/g, respectively.

The type and optimum amount of the alkaline solution can play an important role in activating the slag. Many studies have, therefore, been conducted on alkaline solutions. Usually, sodium hydroxide (NaOH) and sodium silicate (Na₂SiO₃) are used as an alkaline solution for the production of the AAS concrete [27, 28]. The alkali substance can be added to the slag in solid or liquid, but the use of an alkaline solution in the liquid form results in the higher compressive strength, as compared with solids [29]. Sodium hydroxide (NaOH) solution with the concentration of 6 M could provide the highest compressive strength [30]. In this study, a mixture of two types of alkaline solutions including sodium hydroxide (NaOH) and sodium silicate (Na₂SiO₃) was used. Solid sodium hydroxide was dissolved in water with the purity of 98% to obtain the concentration of 6 M. Liquid sodium silicate with the SiO₂/Na₂O ratio of 2.6 (Na₂O = 15%, SiO₂ = 39% and H₂O = 46%) was used too.

The materials used in this study included gravel and mountain crushed sand, in accordance with the ASTM C33 standard [31]. The sand with the fineness modulus of 2.81, the sand value of 76%, the aggregate density of 2.54 g/cm³, the water absorption of 2.86, and the maximum aggregate dimension of 4.75 mm was used. The gravel with the grain size of 4.75 to 12 mm and 12 to 19 mm, the water absorption of 0.88, and the aggregate density of 2.65 g/cm³ was used too. A naphthalene-based superplasticizer (a strong water-reducing agent) in the F category of the ASTM C494 standard [32] was employed as well.

Table 1. The XRF chemical analysis (wt%) of slag and ordinary Portland cement.

Element	CaO	SiO ₂	Al ₂ O ₃	Fe ₂ O ₃	MgO	SO ₃	K ₂ O	Na ₂ O
Slag	38.23	35.43	13.28	0.76	8.74	2.4	0.53	0.47
OPC	64.04	21.52	4.96	3.86	1.61	1.95	-	-

Table 2. Factors used in the mix design.

Factor	Value
alkali solution / slag	0.5
sodium hydroxide / sodium silicate	1
Sodium hydroxide solution concentration (M)	6
Water/ solids	0.35
superplasticizer / slag	0.01
Curing temperature (°C)	23±2

2.2. Mix design

Since the aim of this study was to evaluate the thermal resistance of the alkali-activated slag concrete, all controllable factors affecting AASC were assumed to be constant in all mix designs (Table 2). Accordingly, the mix designs of the alkali-activated slag concrete were considered. Based on the previous research, the optimum ratio of the alkaline solution to slag and also, the NaOH to sodium silicate ratio by mass were equal to 0.5 and 1, respectively [31].

Table 3 shows the mix designs of the alkali-activated slag and normal concrete. The mix designs are presented for a cubic meter of concrete. The ratio of water to solids is the ratio of water to the sum of slag or cement, solid sodium hydroxide, and solid sodium silicate. As it is clear from the mix designs, only slag or cement content varied and all other parameters were changed based on the amount of the slag or cement per cubic meter.

2.3. Mixing and curing

At first, the slag was mixed with the broken mountain aggregates in the mixer and then an alkaline solution containing NaOH and Na₂SiO₃ was added to the mixture. Then, water and superplasticizer were added and the materials were mixed for 4 min. 150 mm cubic molds were filled in two

layers in accordance with the BS 1881 standard [33], and each layer was beaten with 25 strokes. The filled molds were placed for 24 h at room temperature; then the specimens were removed from the molds. The specimens were placed in a water pond with the temperature of 23±2 °C to be cured until the age of 7 and 28 days. It should be noted that three specific cubic concrete specimens were made at each of the desired temperatures, and the average compressive strength and mass loss were considered at that specific temperature as the final result for each concrete.

2.4. Heat treatment

The industrial heat treatment furnace of Nima Esfahan Steel Plant was used for heating the specimens, as shown in Fig. 1. The gas-fired furnace with the thermal capacity up to 1100 °C and a perfectly thermally insulated body was equipped with a high-precision thermocouple to show the internal temperature of the furnace.

The furnace was used for heating the cubic specimens at 200, 400, 600 and 800 °C at a heating rate 2.7 °C/min. The specimens were maintained at each temperature for one hour; then, they were taken out of the furnace. For example, to examine the concrete specimens at 800 °C, first, they were placed in the furnace for 5 hours until the furnace temperature

Table 3. The mix designs of the alkali-activated slag concrete (AASC).

	Mixture	Slag kg/m ³	Sodium hydroxide solution kg/m ³	Sodium silicate solution kg/m ³	Aggregate kg/m ³			Water/Solids	Superplasticizer kg/m ³
					Sand	4.75-12 mm	12-19 mm		
AASC	S300	300	75	75	959	575	384	0.35	3
	S400	400	100	100	846	507	338	0.35	4
	S500	500	125	125	733	440	293	0.35	5
		Cement kg/m ³							
NC	C300	300			1033	620	413	0.35	3
	C400	400			945	567	378	0.35	4
	C500	500			856	514	343	0.35	5



(A) Heat Treatment Furnace



(B) Control Room

Fig. 1. Industrial heat treatment furnace.

reached the temperature of 800°C; next, it was kept at this temperature for one hour, such that the concrete specimens were subject to heat for 6 hours. One hour was devoted to let them reach a steady state; after that, they underwent the cooling process at the ambient temperature. Thus, the specimens were exposed to the temperature rise without an external force to reach the final temperature. The temperature was kept constant for one hour to reach thermal equilibrium. Then, the specimens were cooled. The heating schedule is shown in Fig. 2. The rate of the temperature rise was adjusted according to the amount of the fuel provided to the blower.

2.5. Test methods

2.5.1. Mass loss

One of the important physical properties of concrete is the mass density of concrete. When concrete is exposed to high temperatures, due to evaporation of water in concrete, the mass density of concrete decreases. To evaluate the mass density reduction of concrete, the mass of concrete samples after heat treatment is measured and compared with the concrete mass before heat exposure.

2.5.2. Compressive test

Among the mechanical properties, the study of compressive strength is of particular importance due to its decisive role in

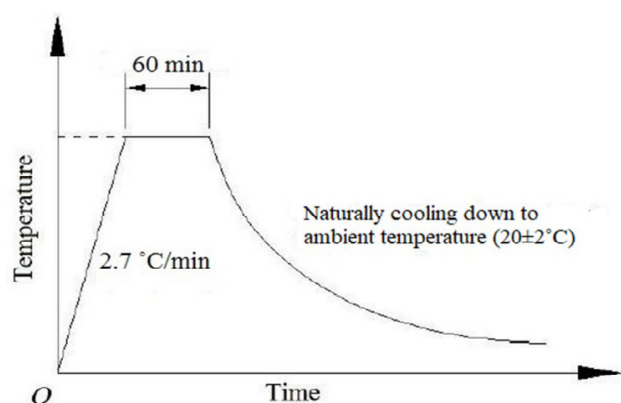


Fig. 2. Heating schedule (schematic view).

the design of structures. Most researchers have pointed to the decrease in this property with increasing temperature [34-36]. However, concrete strength usually gives a general idea of the quality of concrete, due to the fact that strength directly depends on the Binder paste structure. Finally, to evaluate the thermal resistance of AASC, the compressive strength of the specimens was measured at the ambient temperature. The compressive strength was obtained in accordance with the BS 1881 standard [33], by dividing the maximum load applied to the specimens during testing by their cross-sectional area. For this purpose, the dimensions of 150 mm cubic specimens were accurately measured by the caliper. Then, the samples were subjected to continuous loading at a constant speed of 0.25 MPa/sec until their rupture occurred. Three identical samples were tested for each case; the average test results have been reported and discussed in this paper. Fig. 3 shows the cubic specimens of the alkali-activated slag concrete and the normal concrete with Portland cement ruptured under the compressive strength test.

2.5.3. Statistical analysis

The results, presented as mean \pm standard deviation, were analyzed using the T-test method, as well as one-way and two-way ANOVA, by employing the SPSS 16 software. The probability of 0.05 or less was considered statistically significant. It should be noted that the type of concrete, the amount of slag and cement consumed per cubic meter of concrete, and temperature were taken as the independent variables, while the mass loss and compressive strength were considered as the dependent ones.

2.5.4. Scanning electron microscopy (SEM)

Scanning electron microscopy (SEM) was performed on the sample fragments using a Philips XI30 microscope to understand the microstructure of the AAS and the normal concrete. Sample fragments without exposure and with the exposure temperatures of 200, 400, 600 and 800°C were examined by SEM.

2.5.5. Mercury intrusion porosimetry (MIP)

Mercury intrusion porosimetry (MIP) by employing

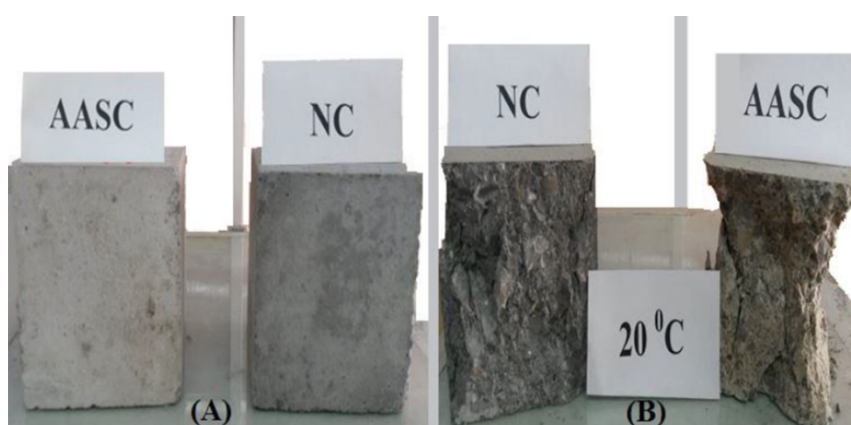


Fig. 3. AASC and NC, (A) before and (B) after compressive strength testing.

Porosimeter PASCAL 140 and Porosimeter PASCAL 440 was conducted to investigation of the change in the structure of the pores of the alkali-activated slag concrete. The sizes of the pores were determined by the pressure required to enter a certain amount of mercury into them.

3. RESULTS AND DISCUSSION

3.1. Visual inspections

The assessment of the fire-damaged concrete usually starts with the visual observation of color change, cracking, and spalling of the concrete surface [37]. Fig. 4 shows the specimens of the alkali-activated slag concrete and the normal concrete under the compressive strength test after placement in the furnace at different temperatures. As the heat applied to the concrete increased, the dark green color that resulted from the slag hydration products began to fade in the AASC samples. Finally, the internal color of the concrete was changed to dark gray at 800°C.

Fig. 5. shows the surface texture of concrete specimens exposed to high temperatures. As the temperature increased,

the number of cracks increased on the surface of the alkali-activated slag concrete and eventually, the size of these cracks was further increased at 800 °C.

Fig. 6 shows the concrete surface of the AAS concrete and the normal concrete at 800°C. As can be seen, on the concrete surface of AASC, there were many cracks resulting from the pressure of the evaporating water and the temperature gradient. On the other hand, throughout the surface of the normal concrete, separation of layers (exfoliation of concrete due to chemical alterations after exposure to high temperatures) was visible. The failure of the heated concrete surface occurred mostly by the cracks formation parallel to the hot surface, degradation of the concrete strength, and pressurization of concrete pores [38]. Furthermore, the concrete can often be broken into pieces without any prior notice due to thermal explosions.

3.2. Mass loss

Mass loss is one of the important changes occurring in the concrete specimens when exposed to the elevated temperatures

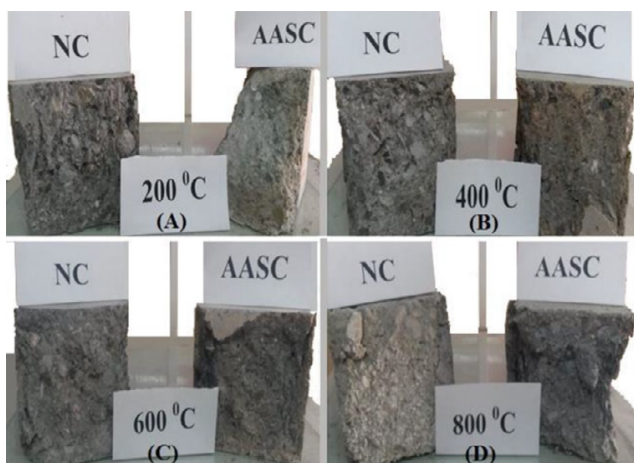


Fig. 4. Specimens of AASC and NC under the compressive strength test after placement in the furnace at (A) 200 °C, (B) 400 °C, (C) 600 °C and (D) 800 °C.

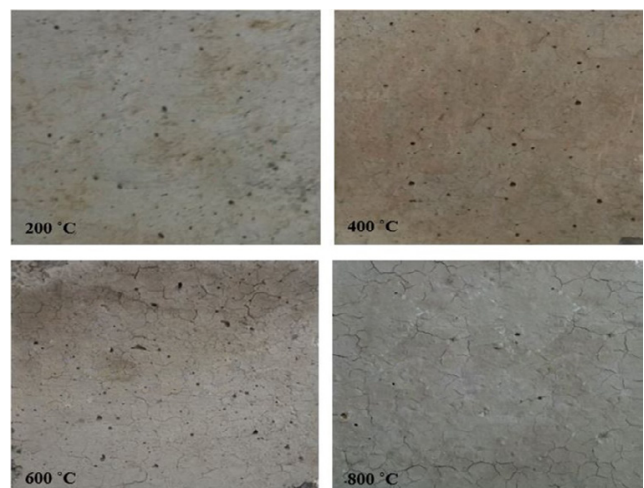


Fig. 5. Surface textures of AASC specimens exposed to high temperatures.



Fig. 6. Surface textures of concrete at 800 °C.

due to water evaporation in concrete. The mass loss of cubic specimens (mass loss percentage is obtained by dividing the mass difference of the heated and unheated specimens by the mass of the unheated specimens) was obtained after the heat treatment and removal from the furnace. Fig. 7 shows the mass loss in both types of concrete due to the exposure to different temperatures. As can be seen, as the temperature was increased, the mass of the cubic AASC and normal concrete specimens was decreased around 10.5% and 13% at 800°C, respectively. The mass of all concrete types with different mix designs was decreased with a gentle slope from 20 to 800°C, showing the relative match of different mix designs.

Generally, the mass loss occurring with increasing temperature from the ambient one to 200°C could be due to the elimination of the evaporable water and the removal of free water in the capillary pores. The mass loss at 400°C was due to the elimination of water in the chemical bonds due to the decomposition of carboaluminate hydrates. Mass loss was inevitable because of the breakdown of most bonds in the C-A-S-H silicate gel at temperatures above 600°C. According to Fig. 7, the mass of AASC was decreased with a gentle slope

from 20 to 800°C. But, the mass of the normal concrete was decreased with a gentle slope up to 600°C; then, the mass was decreased with a steep slope from 600 to 800°C. This could represent the significant degradation of the microstructure of the normal concrete with Portland cement at 800°C.

3.3. Compressive strength

The compressive strength of cubic specimens with the dimensions of 150 × 150 × 150 mm was measured after curing in a water pond and placement in the air in accordance with the BS 1881 standard. Fig. 8 shows the compressive strength of the alkali-activated slag concrete and the normal concrete with Portland cement.

As can be clearly seen from the results brought in Fig. 8, the compressive strength of concrete was increased at all ages with enhancing the slag and cement content. The reason for this enhanced strength in both types of concrete was that with increasing the binder material, the production of the C-A-S-H gel in AASC and C-S-H in NC, as the main factor influencing the concrete strength, was enhanced. On the other hand, with increasing the binder material, the concrete structure became

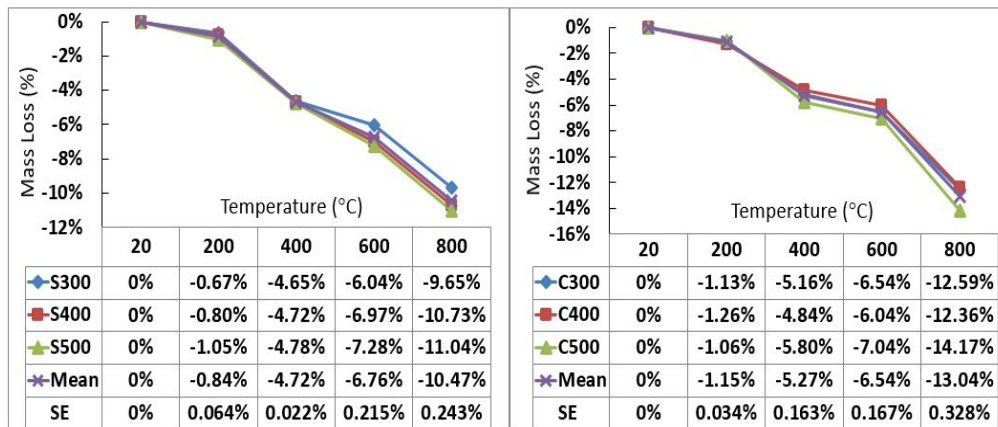


Fig. 7. Mass loss (%) of AASC and NC at different temperatures.

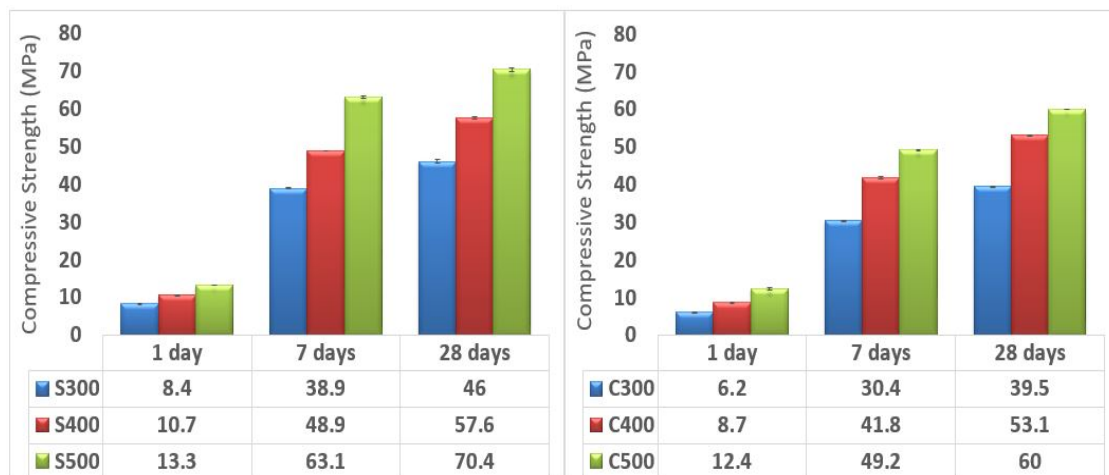


Fig. 8. Compressive strength of AASC and NC at the ages of 1, 7 and 28 days.

denser and pores in the concrete were reduced.

Comparing the compressive strength of the 1 and 28-day alkali-activated slag concrete and the normal concrete with Portland cement showed that the compressive strength of the former was higher than that of latter with the same grade. On average, the 1-day and 28-day strength of the alkali-activated slag concrete was 1.22 and 1.15 times more than that of the normal concrete, respectively. This could be attributed to several reasons including the finer structure of the slag, as compared with the normal Portland cement (slag and cement Blaine were equal to 4500 and 3270 cm²/g, respectively), leading to the denser and less porous structure of ASSC, as compared with the normal concrete. On the other hand, the presence of an alkaline solution of sodium silicate in AASC as a source of silica (SiO₂) enhanced C-A-S-H gel production, leading to the increased compressive strength.

Compressive strength is the most important mechanical property examined with increasing temperature. As it is evident from the results in Fig. 9, the compressive strength of

all specimens was enhanced with increasing the slag content at all temperatures. Notably, the compressive strength of AASC, on average, was decreased about 25% up to 600°C. This showed the higher thermal resistance of the alkali-activated slag, as compared with the normal concrete, such that it retained more than 70% of the compressive strength up to 600°C. The compressive strength of AASC was significantly decreased from 600 to 800°C, such that about 70% of the compressive strength was reduced. The compressive strength was decreased with a gentle slope from 20 to 600°C, but a sharp decline was observed in the compressive strength from 600 to 800°C.

According to the variations in the compressive strength of the normal concrete with temperature (Fig. 10), the compressive strength of the specimens was raised at all temperatures with increasing the cement content. However, the compressive strength was decreased with a gentle slope up to 400°C; then, it was decreased sharply from 400 to 800°C. About 52% of the compressive strength of the normal

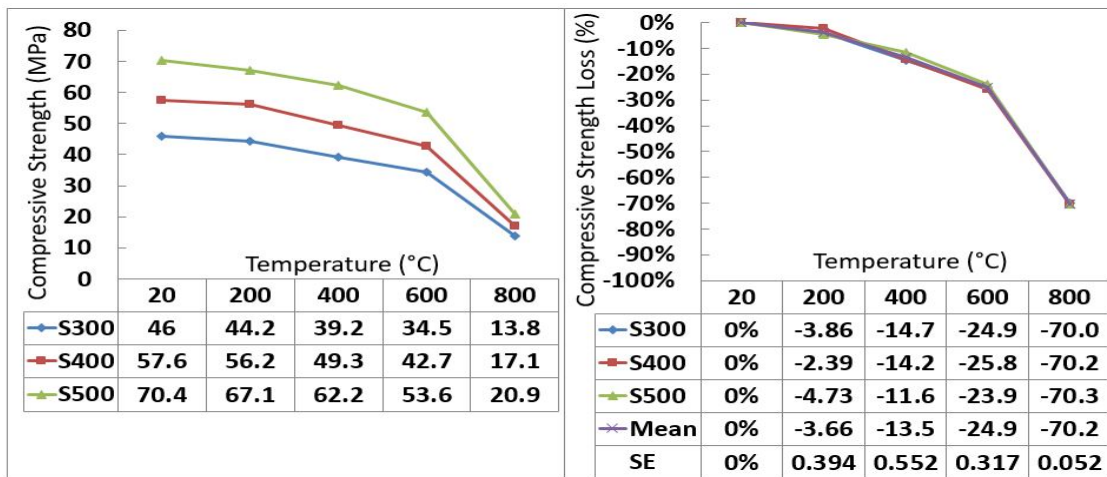


Fig. 9. Compressive strength of the 28-day AASC at different temperatures.

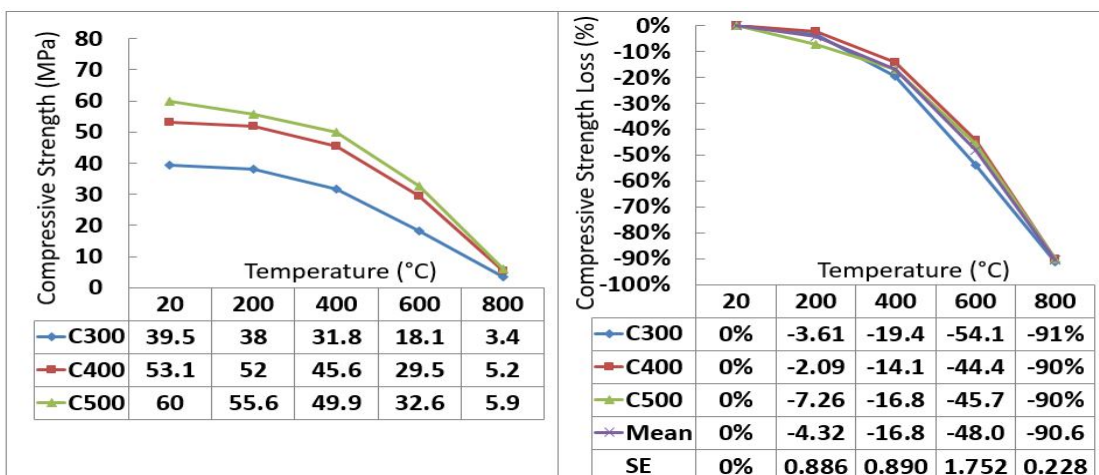


Fig. 10. Compressive strength of the 28-day NC at different temperatures.

concrete was retained at 600°C. However, around 10% of the compressive strength remained at 800°C.

Comparing the results of AASC with those of the normal concrete with Portland cement showed that the AASC displayed higher compressive strength in comparison to the normal concrete. The alkali-activated slag concrete retained about 75% and 30% of its compressive strength up to 600 and 800°C, respectively. Generally, compressive strength was decreased with increasing the temperature due to the reduction in the chemically bonded water because of the dehydration and the partial decomposition of C-A-S-H. The coarse pores structure and the complete dehydration at elevated temperatures, as well as the removal of water from the hydrated pores to the extent that happened in the first stage of dehydration, could be noted as other reasons. On the other, the decomposition of C-A-S-H gel at temperatures above 600°C is the main cause of the significant decrease in compressive strength of concrete.

3.4. Statistical analysis

3.4.1. T-test

T-test was used to evaluate the effect of the concrete type on the mass and compressive strength loss of concrete specimens at different temperatures. According to Table 4, the results could not be considered for the effect of the type of concrete on the reduction of mass until reaching the temperature of 600°C. On the other hand, the difference in the type of concrete was

significant at 800°C ($P_{800} = 0.02$) and it could be concluded that the AASC concrete had less mass loss, as compared to that of the normal concrete. At 200 and 400°C, the compressive strength loss mean in the two types of concrete was not significantly different ($P_{200} = 0.71$, $P_{400} = 0.15$). So, at 600 and 800°C, according to the results of the experiments, it could be concluded that the AASC concrete had less compressive strength loss in comparison to the normal concrete.

3.4.2. ANOVA test

One-way ANOVA was used to study the effect of temperature variations on the reduction of the AASC and normal concrete mass and compressive strength. According to the results brought in Table 5, there was a significant difference in both types of concrete at different temperatures ($P = 0.001$). This showed that the independent variable of temperature had a significant effect on the mass and compressive strength loss of the specimens; as it is evident, the mass and compressive strength of the concrete specimens was decreased with increasing the temperature.

The effect of the amount of slag and cement consumed per cubic meter of concrete was studied using one-way ANOVA. The results showed that the difference in the mean values was non-significant, changing the amount of the slag and cement consumed per cubic meter could have no effect on reducing the specimens' mass and compressive strength of the concrete (Table 6).

Table 4. The effect of the concrete type on mass and compressive strength loss at different temperatures.

Temp. (°C)	mass loss			compressive strength loss		
	t	P	Effect	t	P	Effect
200	-2.46	0.07	non-significant	-0.39	0.71	non-significant
400	-1.93	0.13	non-significant	-1.79	0.15	non-significant
600	0.47	0.66	non-significant	-7.50	0.002	significant
800	-3.63	0.02	significant	-58.26	0.001	significant

Table 5. The effect of temperature changes on the mass and compressive strength loss of AASC and NC specimens.

Concrete Type	mass loss			compressive strength loss		
	F	P	Effect	F	P	Effect
AASC	282.00	0.001	significant	2.286E3	0.001	significant
NC	272.19	0.001	significant	505.416	0.001	significant

Table 6. The effect of the amount of slag and cement consumed per cubic meter of concrete on the mass and compressive strength loss of concrete specimens at different temperatures.

	N	Mean± The standard deviation	F	P	Effect	Mean± The standard deviation	F	P	Effect
AASC	S300	5	4.20±3.98	0.03	0.97	non-significant	22.72±28.20	0.001	non-significant
	S400	5	4.64±4.44				22.56±28.60		
	S500	5	4.83±4.53				22.14±28.42		
NC	C300	5	5.08±5.00	0.03	0.98	non-significant	33.64±38.55	0.011	non-significant
	C400	5	4.90±4.85				30.13±37.88		
	C500	5	5.61±5.65				31.96±36.80		

Regarding the results of T-test and one-way ANOVA, it was determined that the two independent variables of concrete type and temperature were effective on reducing the concrete specimens' mass and compressive strength. Two-way ANOVA was performed to examine the simultaneous effect of these two independent variables. As shown in Fig. 11, with increasing the temperature, the reduction in the mass and compressive strength of both types of concrete was intensified. The distance between the temperature lines indicated the difference in the mass and compressive strength

loss at different temperatures. By observing the slope of the temperature lines, it was evident that, due to the low slope of these lines at the temperatures of 20, 200, 400 and 600 °C, the type of concrete at these temperatures had no effect on the reduction of the mass of the concrete specimens. However, given the slope of the 800 °C temperature line, it was clear that at this temperature, the type of concrete had no effect on the reduction of mass, and the AASC had less mass loss in comparison to NC. On the other hand, by observing the slope of the temperature lines, it was evident that, due to

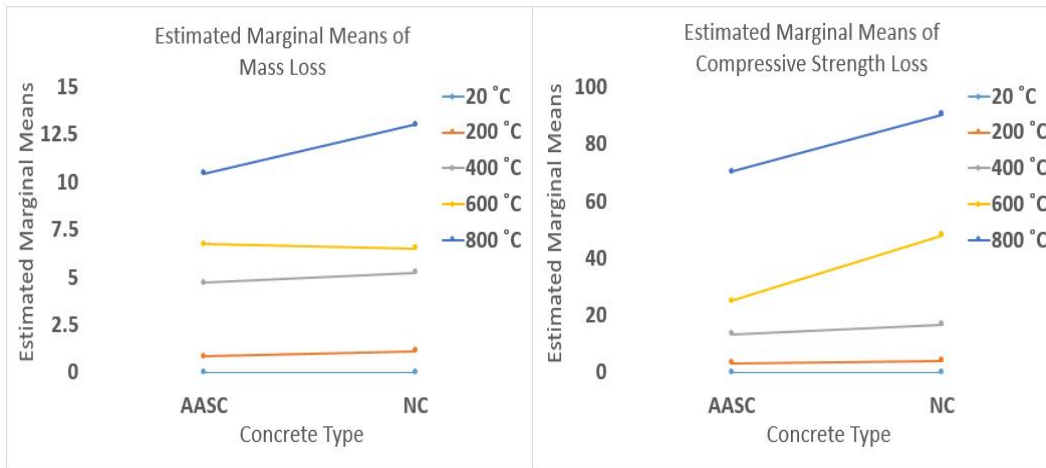


Fig. 11. The simultaneous effect of the two independent variables of concrete type and temperature on the mass and compressive strength loss of the concrete specimens.

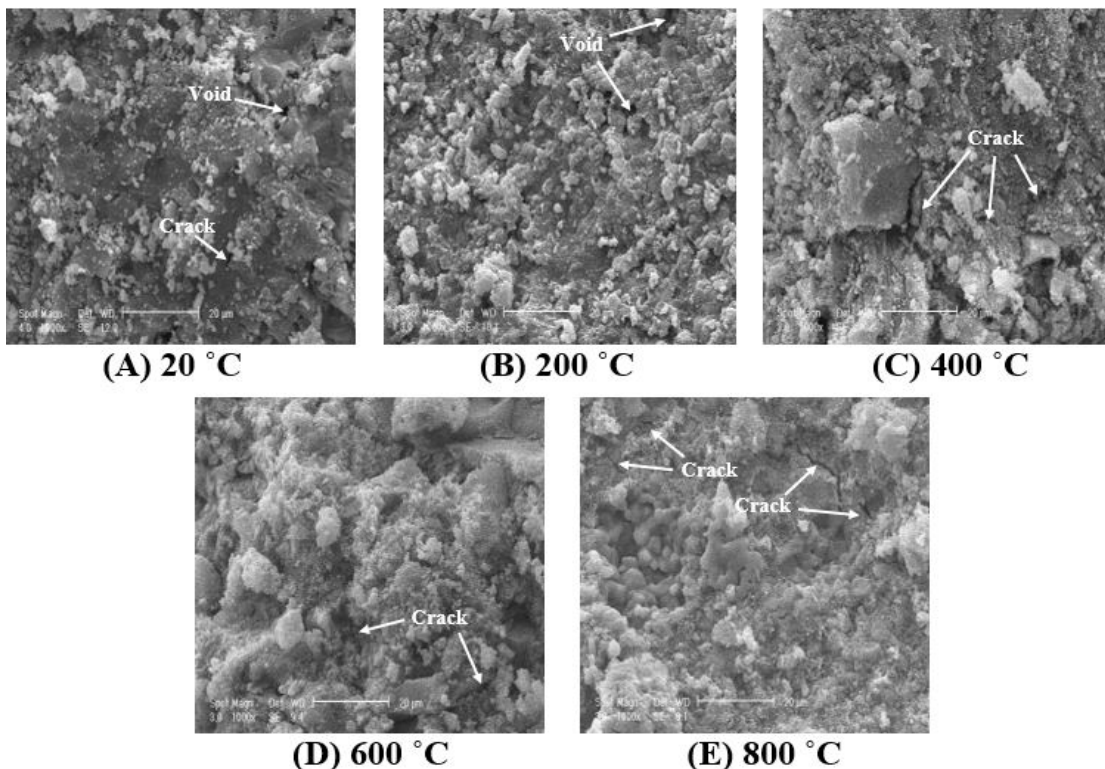


Fig. 12. Micrographs of AASC at different temperatures (scale: 20 µm).

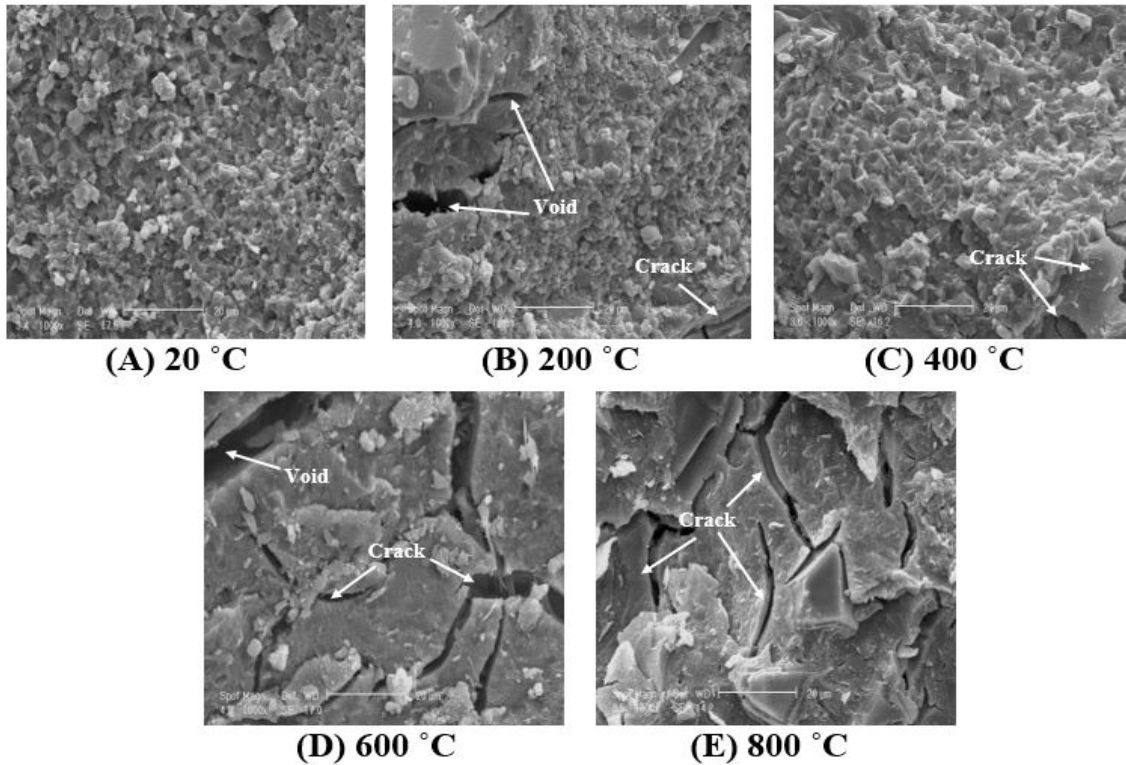


Fig. 13. Micrographs of NC at different temperatures (scale: 20 µm).

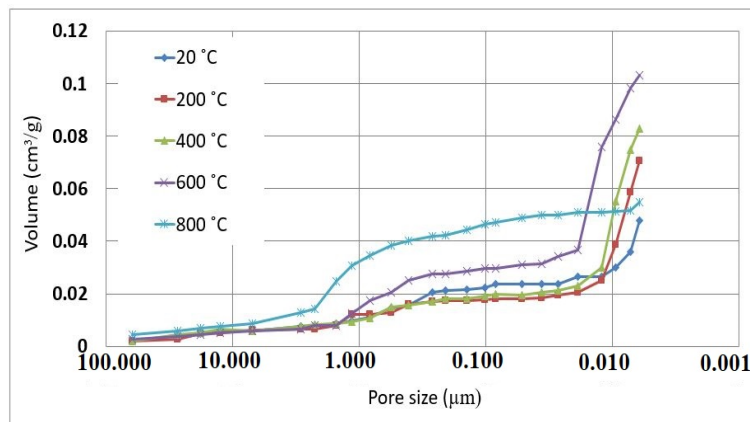


Fig. 14. The pores size of AASC at different temperatures.

the low slope of these lines at the temperatures of 20, 200 and 400°C, the type of concrete at these temperatures had no effect on the reduction of the compressive strength of the concrete specimens. However, according to the slope of the 600 and 800°C temperature lines, it was clear that at these temperatures, the type of concrete had an effect on the reduction of the compressive strength, and the AASC had less compressive strength loss in comparison to the NC.

3.5. Scanning electron microscopy (SEM)

Scanning electron microscopy were used to compare the microstructures of the AASC concrete and the normal

concrete with Portland cement at different temperatures. Fig. 12 shows the electron microscopy photographs (scale: 20 µm) of the alkali-activated slag concrete. As can be clearly seen from Fig. 12-A, The AASC has a large number of microcracks due to rapid initial setting time. According to Fig. 12-B and C, fine cracks were formed in the structure of the C-A-S-H gel because of the pores water pressure, and the decomposition and further shrinkage of the binder, which could be correlated with a considerable decrease in the compressive strength. As can be seen in Fig. 12-D, the number and depth of the cracks in the paste were increased due to the evaporation of the chemically bonded water. Fig. 12-E shows the significant

rupture of the C-A-S-H gel, leading to a sharp reduction in the compressive strength. It also appeared that the crystalline structure of the concrete was changed by varying the temperature from 600 to 800 °C.

Fig. 13 shows the SEM (20 µm) of the normal concrete. Comparing Fig. 12 and Fig. 13 showed structural differences between these two types of concrete. As it is evident in Fig. 13-A, the normal concrete structure at room temperature was composed of C-S-H and calcium hydroxide (CH) crystals. According to Fig. 13-B, no significant changes were observed in the paste except very small cracks due to pore water pressure. As can be observed in Fig. 13-C, fine cracks were formed with increasing the temperature because of the removal of the chemically bonded water by dehydration. As shown in Fig. 13-D, it is evident that the CH crystals were converted to calcium oxide and also cracks were reached the concrete surface due to the completion of the dehydration process and the decomposition of the C-S-H gel. At temperatures up to 600 °C, these cracks were increased dramatically, resulting in a sharp drop in the compressive strength at this temperature. With the almost complete destruction of the C-S-H gel as the main factor influencing the concrete strength, the compressive strength of concrete was significantly decreased, as shown in Fig. 13-E.

3.6. Pores structure

Fig. 14 shows the results of the MIP test on the alkali-activated slag concrete that indicating a change in the pores structure of the AASC with increasing heat. The number and size of cracks in the alkali-activated slag concrete were enhanced with increasing temperature up to 600 °C. At 800 °C, the pores size became very large and varies from 0.1 to 10 µm. This sharp increase in crack size from 600 to 800 °C is the main cause of the severe decrease in compressive strength of AASC.

4. CONCLUSION

In this study, the effect of temperature on the performance of the alkali-activated slag concrete was studied. The mass loss and compressive strength variations of the AAS concrete specimens containing varying amounts of the blast furnace slag were measured after subjecting them to the temperatures of 200, 400, 600 and 800 °C. Changes in the microstructure and porosity of the binder paste due to the high temperature were also studied by scanning electron microscopy (SEM) images and mercury intrusion porosimetry (MIP), respectively. The results could contribute to the application of the alkali-activated slag (AAS) concrete as an approach useful for the production of the environmentally-friendly green concrete. The main results of this study could be summarized here:

The compressive strength of AASC was enhanced from 46 to 70.4 MPa with increasing the slag content of the alkali-activated slag concrete from 300 to 500 Kg/m³ while keeping constant other factors influencing the mix design, such as the ratio of the alkali activator to slag, the ratio of sodium hydroxide to sodium silicate, the ratio of water to solids, and the percentage of the superplasticizer used.

The compressive strength of the alkali-activated slag concrete was higher than that of the normal concrete with Portland cement and the same mix design. The compressive strength of the 28-day alkali-activated slag concrete was, respectively, 1.15 times more than that of the normal concrete.

The mass loss of the concrete specimens was enhanced with increasing the temperature. The mass loss of the alkali-activated slag concrete with increasing temperature was less than that of the normal concrete with Portland cement. The mass reduction of the alkali-activated slag concrete cubic specimens was about 2.5% less than that of the normal concrete. The average percentage of mass reduction in the cubic specimens of the AAS concrete was 10.5%, while in the normal one, it was 13%.

The compressive strength of concrete was decreased with increasing the temperature. With increasing the temperature to 800 °C, the compressive strength of the alkali-activated slag concrete and the normal concrete with Portland cement was decreased by 70% and 90%, respectively.

The results of the statistical analysis conducted with T-test and ANOVA showed that the independent variables of concrete type and temperature were effective on the dependent variables of the mass loss and compressive strength of the concrete; the mean variables were significant too; on the other hand, the independent variable of the amount of the slag and cement consumed in each concrete cubic meter had no effect on the dependent variables, such that the mean variations were non-significant.

The results of the statistical analysis carried out by T-test and ANOVA showed that up to 600 °C, the concrete type had no effect on the reduction of the concrete specimens mass; however, at the temperature of 800 °C, the effect of the concrete type on the reduction of mass was evident, such that the mass loss of AASC was less than that of NC. On the other hand, up to 400 °C, the concrete type had no effect on reducing the compressive strength; nevertheless, at 600 and 800 °C, the effect of the independent variable of concrete type on the reduction of compressive strength was evident. At the temperatures of 600 and 800 °C, the compressive strength loss of NC was higher than that of AASC.

With increasing the temperature, the cracks appeared on the surface of the AASC. At 600 °C, these cracks were clearly visible. The development of these cracks and drastic increase in size of cracks up to 10 µm at 800 °C caused the complete rupture of the C-A-S-H gel and the reduction of the compressive strength of concrete.

The thermal resistance of the alkali-activated slag concrete was higher than that of the normal concrete with Portland cement. In general, the alkali-activated slag concrete showed a very good thermal performance.

REFERENCES

- [1] Y. Ding, J.G. Dai, C.J. Shi, Mechanical properties of alkali-activated concrete: A state-of-the-art review, *Construction and Building Materials*. 127 (2016) 68-79.
- [2] J.L. Provis, Geopolymers and other alkali activated materials: why, how, and what?, *Materials and Structures*. 47 (2014) 11-25.
- [3] J. Davidovits, *Geopolymer chemistry and applications*, Geopolymer

- Institute 2015.
- [4] C. Shi, D. Roy, P. Krivenko, Alkali-activated cements and concretes, CRC press 2006.
- [5] K. Behfarnia, M. Hasanzade, Advanced topics in cement and pozzolan: technology, Jahād-e Dāneshgāhi of Isfahan. (2014).
- [6] M. Rostami, K. Behfarnia, The effect of silica fume on durability of alkali activated slag concrete, *Construction and Building Materials*. 134 (2017) 262–268.
- [7] J.L. Provis, S.A. Bernal, Geopolymers and related alkali-activated materials, *Annual Review of Materials Research*. 44 (2014) 299-327.
- [8] Z. Pan, J.G. Sanjayan, Stress-strain behaviour and abrupt loss of stiffness of geopolymer at elevated temperatures, *Cement and Concrete Composites*. 32(9) (2010) 657-664.
- [9] Z. Pan, J.G. Sanjayan, F. Collins, Effect of transient creep on compressive strength of geopolymer concrete for elevated temperature exposure, *Cement and Concrete Research*. 56 (2014) 182-189.
- [10] Z. Pan, J.G. Sanjayan, B.V. Rangan, An investigation of the mechanisms for strength gain or loss of geopolymer mortar after exposure to elevated temperature, *Journal of Materials Science*. 44(7) (2009) 1873-1880.
- [11] M. Guerrieri, J. Sanjayan, F. Collins, Residual compressive behavior of alkali-activated concrete exposed to elevated temperatures, *Fire and Materials*. 33(1) (2009) 51-62.
- [12] R. Zhao, J.G. Sanjayan, Geopolymer and Portland cement concretes in simulated fire, *Magazine of Concrete Research*. 63(3) (2011) 163-173.
- [13] D.L. Kong, J.G. Sanjayan, Damage behavior of geopolymer composites exposed to elevated temperatures, *Cement and Concrete Composites*. 30(10) (2008) 986-991.
- [14] D.L. Kong, J.G. Sanjayan, Effect of elevated temperatures on geopolymer paste, mortar and concrete, *Cement and Concrete Research*. 40(2) (2010) 334-339.
- [15] D.L. Kong, J.G. Sanjayan, K. Sagoe-Crentsil, Comparative performance of geopolymers made with metakaolin and fly ash after exposure to elevated temperatures, *Cement and Concrete Research*. 37(12) (2007) 1583-1589.
- [16] İ. Türkmen, M.B. Karakoç, F. Kantarcı, M. M. Maraş, R. Demirboğa, Fire resistance of geopolymer concrete produced from Elazığ ferrochrome slag, *Fire and Materials*. 40(6) (2016) 836-847.
- [17] T. Bakharev, Thermal behaviour of geopolymers prepared using class F fly ash and elevated temperature curing, *Cement and Concrete Research*. 36 (2006) 1134-1147.
- [18] T.W. Cheng, J.P. Chiu, Fire-resistant geopolymer produced by granulated blast furnace slag, *Minerals Engineering*. 16 (2003) 205–210.
- [19] I. Giannopoulou, D. Paniás, Fire Resistant geopolymers synthesized from industrial wastes, *World Journal of Engineering*. 5 (2008) 130-131.
- [20] Z. Pan, Z. Tao, Y.F. Cao, R. Wührer, T. Murphy, Compressive strength and microstructure of alkali activated fly ash/slag binders at high temperature, *Cement and Concrete Composites*. 86 (2018) 9-18.
- [21] F. Aslani, Z. Asif, Properties of Ambient-Cured Normal and Heavyweight Geopolymer Concrete Exposed to High Temperatures, *Materials*, 12(5) (2019) 740.
- [22] K. Behfarnia, M. Shahbaz, The effect of elevated temperature on the residual tensile strength and physical properties of the alkali-activated slag concrete, *Journal of Building Engineering*. 20 (2018) 442–454.
- [23] Y.L. Li, X.L. Zhao, R.K. Singh Raman, S. Al-saadi, Thermal and mechanical properties of alkali-activated slag paste, mortar and concrete utilising seawater and sea sand, *Construction and Building Materials*. 159 (2018) 704-724.
- [24] The American Society for Testing and Materials, Standard specification for ground granulated blast furnace slag for use in concrete and mortars, ASTM C989. Vol.04.02 (2013).
- [25] B. Talling, J. Brandstet, Present state and future of alkali-activated slag concretes, *ACI Special Publication*. 114 (1989).
- [26] J. Chang, A study on the setting characteristics of sodium silicate-activated slag pastes, *Cement and Concrete Research*. 33 (2003) 1005-1011.
- [27] D. Hardjito, S.E. Wallah, D.M.J. Sumajouw, B.V. Rangan, On the development of fly ash-based geopolymer concrete, *ACI Materials Journal*. 101(6) (2004) 467-472.
- [28] S. Aydin, B. Baradan, Mechanical and microstructural properties of heat cured alkali-activated slag mortars, *Materials and Design*. 35 (2012) 374–383.
- [29] S.D. Wang, K.L. Scrivener, P.L. Pratt, Factors affecting the strength of alkali activated slag, *Cement and Concrete Research*. 24(6) (1994) 1033-1043.
- [30] M. Shojaei, K. Behfarnia, R. Mohebi, Application of alkali-activated slag concrete in railway sleepers, *Materials and Design*. 69 (2015) 89–95.
- [31] The American Society for Testing and Materials, Standard specification for concrete aggregates, ASTM C33. Vol.04.02 (2003).
- [32] The American Society for Testing and Materials, Standard specification for chemical admixtures for concrete, ASTM C494. Vol.04.02 (2003).
- [33] BS 1881: part 5, Testing concrete: Methods of testing hardened concrete for other than strength, British Standard Institution. London. (1970).
- [34] EN 1992-1-2. Eurocode 2: Design of concrete structures- Part 1-2: General rules- Structural fire design, 97 (2004).
- [35] M. Talha Junaid, A. Khennane, O. Kayali, A. Sadaoui, D. Picard, M. Fafard, Aspects of the deformational behaviour of alkali activated fly ash concrete at elevated temperatures, *Cement and Concrete Research*. 60 (2014) 24-29.
- [36] W. Khaliq, H. Anis Khan, High temperature material properties of calcium aluminate cement concrete, *Construction and Building Materials*. 94 (2015) 475-487.
- [37] B. Georgali, P.E. Tsakiridis, Microstructure of fire-damaged concrete, *Cement and Concrete Composites*. 27 (2005) 255-259.
- [38] K. Sakr, E. El-Hakim, Effect of high temperature or fire on heavy weight concrete properties, *Cement and Concrete Research*. 35 (2005) 590-596.

HOW TO CITE THIS ARTICLE

M. Shahbaz, K. Behfarnia, *Thermal strength of the alkali-activated slag concrete*, *AUT J. Civil Eng.*, 4(3) (2020) 303-314.

DOI: [10.22060/ajce.2019.16793.5601](https://doi.org/10.22060/ajce.2019.16793.5601)

